

Electrochemical potential tuned solar water splitting

Stuart Licht,^{*a} Leonid Halperin,^b Michael Kalina,^b Martina Zidman^{ab} and Nadezhda Halperin^b

^a Department of Chemistry, University of Massachusetts Boston, Boston, 32000, USA.

E-mail: stuart.licht@umb.edu; Fax: 617-287-6030; Tel: 617-287-6156

^b Department of Chemistry, Technion Israel Institute of Technology, Haifa, 32000, ISRAEL

Received (in Cambridge, UK) 7th August 2003, Accepted 20th October 2003

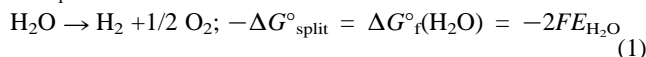
First published as an Advance Article on the web 7th November 2003

As a fundamental step towards a clean, renewable source of H₂, a novel physical chemical process within molten NaOH in which an external single, small band gap photosensitizer, such as Si, can drive the energetics of water cleavage is demonstrated, and is accomplished by tuning (decreasing) the water splitting electrochemical potential, $E_{\text{H}_2\text{O}}$, rather than tuning the photosensitizer band gap; this diminished potential is due to (i) a thermodynamic temperature induced decrease of $E_{\text{H}_2\text{O}}$ with increasing temperature, and (ii) a partial recombination of the cleavage products.

Solar water splitting can provide clean, renewable sources of hydrogen fuel. However, direct^{1a} or indirect thermochemical,^{1b} biological,^{2a} or photochemical,^{2b} solar water splitting has generally driven low rates of water splitting with the best results achieved with semiconductors as photosensitizers,^{3–5} with up to 18% efficiency observed.⁶ Utilizing solar heat to facilitate water electrolysis had been suggested,⁷ although no rigorous analysis from the fundamentals of solar energy, thermodynamics and electrochemical processes had been developed. Recently, a novel model for electrochemical solar water splitting processes by semiconductor materials was presented with the first derivation of band gap restricted thermal enhanced solar water splitting efficiencies.⁸ The model provides a theoretical basis for solar energy to hydrogen conversion efficiencies in the 50% range, by combing excess sub-bandgap insolation with efficient solar driven water electrolysis at elevated temperatures.

Studies had focused on diminishing the high band gap apparently required for solar water splitting.^{3,4} Semiconductors, such as TiO₂ can split water, but their wide bandgap limits the photo response to a small fraction of the incident solar energy. Studies sought to improve the solar water splitting by tuning (decreasing) the bandgap of the photosensitizers, E_g , to better match the water splitting potential, $E_{\text{H}_2\text{O}}$. In this experimental study, we take an alternate approach: instead of tuning E_g to fit $E_{\text{H}_2\text{O}}$, we tune $E_{\text{H}_2\text{O}}$ to fit E_g . We probe an unexpected physical chemical process in which the potential for water splitting diminishes in molten NaOH to below the expected thermodynamic value. The result is H₂ evolution at potentials compatible with existing efficient smaller band gap photovoltaics, such as Si, and at sufficiently low temperatures (500 °C) to not pose substantial material constraints.

Fig. 1 includes the variation of $E_{\text{H}_2\text{O}}$ with temperature and pressure, calculated from the free energy of formation, ΔG_f° :



Reaction 1 is endothermic, and without external heat cools water. The enthalpy balance and thermoneutral potential, E_{tneut} , are:

$$-\Delta H_{\text{split}}^\circ = \Delta H_f(\text{H}_2\text{O}_{\text{liq}}); E_{\text{tneut}} \equiv -\Delta H_f(\text{H}_2\text{O}_{\text{liq}})/2F \quad (2)$$

Due to overpotential, ζ , and IR losses, the necessary applied electrolysis potential, $V_{\text{H}_2\text{O}}(T)$, is greater than $E_{\text{H}_2\text{O}}^\circ(T)$:

$$V_{\text{H}_2\text{O}}(T) = E_{\text{H}_2\text{O}}^\circ(T) + \zeta_{\text{anode}}(\text{O}_2) + \zeta_{\text{cathode}}(\text{H}_2) + V_{\text{IR}} \quad (3)$$

Fletcher, repeating the fascinating suggestion of Brown that saturated aqueous NaOH will never boil, hypothesised that a useful medium for water electrolysis might be very high

temperature NaOH saturated, aqueous solutions. These do not reach a temperature at which they boil at 1 atm due to the high salt solubility, binding solvent, and changing saturation vapour pressure, as reflected in their phase diagram.⁹ We measure this domain, and also electrolysis in an even higher temperature domain above which NaOH melts (318 °C) creating a molten electrolyte with dissolved water, resulting in unexpected $V_{\text{H}_2\text{O}}$.

Fig. 2 summarizes measured $V_{\text{H}_2\text{O}}(T)$ in aqueous saturated and molten NaOH electrolytes. As seen in the inset, Pt exhibits low overpotentials to H₂ evolution, and is used as a convenient quasi-reference electrode in the measurements which follow. As also seen in the inset, Pt exhibits a known large overpotential to O₂ evolution as compared to a Ni electrode or to $E^\circ\text{H}_2\text{O}(25^\circ\text{C}) = 1.23$ V. This overpotential loss diminishes at moderately elevated temperatures, and as seen in the main portion of the figure, at 125 °C there is a 0.4 V decrease in the O₂ activation potential at a Pt surface. Through 300 °C in Fig. 2, measured $V_{\text{H}_2\text{O}}$ remains greater than the calculated thermodynamic rest potential. Unexpectedly, $V_{\text{H}_2\text{O}}$ at 400 °C and 500 °C in molten NaOH occurs at values substantially smaller than that predicted. These measured values include voltage increases due to IR and hydrogen overpotentials and hence provide an upper bound to the unusually small electrochemical potential. This phenomena is summarized in Fig. 1, in which even at relatively large rates of water splitting (30 mA cm⁻²) at 1 atm, a measured $V_{\text{H}_2\text{O}}$ below that predicted by theory is observed at temperatures above the NaOH melting point. As seen in the figure, the observed value at high temperature of $V_{\text{H}_2\text{O}}$ approaches that calculated⁸ for a thermodynamic system of 500 bar, rather than 1 bar, H₂O.

A source of the nominally less than thermodynamic water splitting potentials is described in Scheme 1. Shown on the left hand is the single compartment cell utilized here. Cathodically generated H₂ is in close proximity to the anode, while anodic O₂ is generated near the cathode. Their presence will facilitate the water forming back reaction, and at the electrodes this recombination will diminish the potential. In addition to the

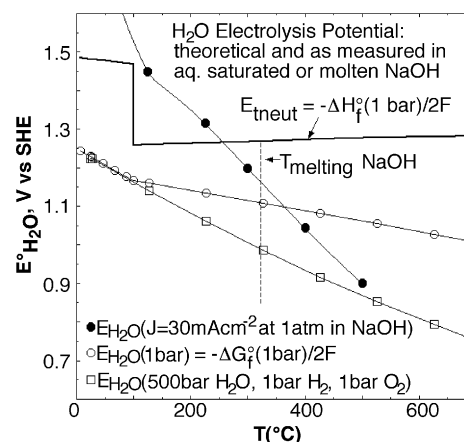


Fig. 1 Thermodynamic $E_{\text{H}_2\text{O}}$ values compared to measured $V_{\text{H}_2\text{O}}(30 \text{ mA cm}^{-2})$ in aq. saturated or molten NaOH. $V_{\text{H}_2\text{O}}$, detailed in Fig. 2.

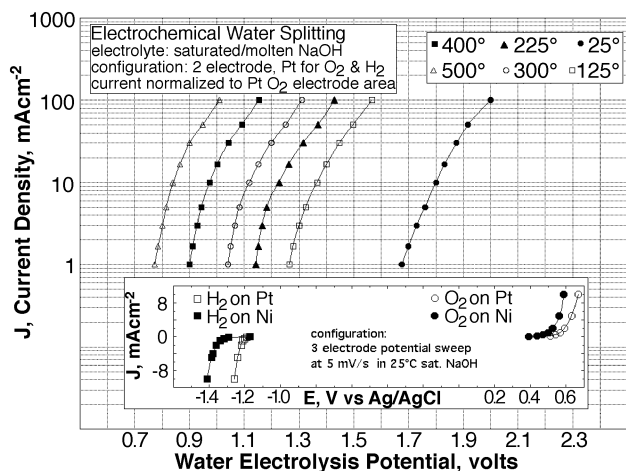
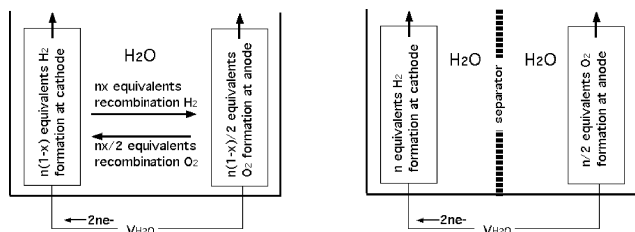


Fig. 2 $V_{\text{H}_2\text{O}}$, measured in aq. saturated or molten NaOH, at 1 atm. CO_2 is excluded by argon purge. The molten electrolyte is prepared from heated, solid NaOH with steam injection. O_2 anode is 0.6 cm^2 Pt foil. IR and polarization losses are minimized by sandwiching 5 mm from each side of the anode, two interconnected Pt gauze (200 mesh , $50 \text{ cm}^2 = 5 \text{ cm} \times 5 \text{ cm} \times 2 \text{ sides}$) cathodes. Fig. inset: At 25° , 3 electrode values at 5 mV s^{-1} versus Ag/AgCl, with either 0.6 cm^2 Pt or Ni foil, and again separated 5 mm from two 50 cm^2 Pt gauze acting as counter electrodes.



Scheme 1 Interelectrode recombination can diminish $V_{\text{H}_2\text{O}}$ and occurs in open (left), but not in isolated (right), configurations; such as examined with or without a Zr_2O_3 mix fiber separator (ZYK-5H, from Zircar Zirconia, FL, NY) situated between the Pt anode and cathodes.

observed low potentials, two observations support this recombination effect. The generated H_2 and O_2 is collected, but is consistent with a coulombic efficiency of $\approx 50\%$ (varying with T , j , and interelectrode separation). Consistent with the right hand side of Scheme 1, when conducted in separated anode/cathode compartments, this observed efficiency is $98\text{--}100\%$. Here, however, all cell open circuit potentials increase to beyond the thermodynamic potential, and at $j = 100 \text{ mA cm}^{-2}$ yields measured $V_{\text{H}_2\text{O}}$ values of 1.45, 1.60, 1.78 V at 500, 400, and 300°C , which are approximately 450 mV higher than the equivalent Fig. 2 values for the single compartment configuration cell.

The recombination phenomenon offers advantages (low $V_{\text{H}_2\text{O}}$), but also disadvantages (H_2 losses), requiring study to balance these competing effects to optimize energy efficiency. In molten NaOH, the effects of temperature variation of $\Delta G_f^\circ(\text{H}_2\text{O})$ and the recombination of the water splitting products can have a pronounced effect on solar driven electrolysis. As compared to 25°C , in Fig. 2 only half the potential is required to split water at 500°C , over a wide range of current densities.

As we have recently demonstrated, the unused thermal photons which are not required in semiconductor photodriven charge generation, can contribute to heating water to facilitate electrolysis at an elevated temperature. The characteristics of one, two, or three series interconnected solar visible efficient photosensitizers, in accord with the manufacturer's calibrated standards, are presented in Fig. 3. These silicon photovoltaics are designed for efficient photoconversion under concentrated insolation ($\eta_{\text{solar}} = 26.3\%$ at 50 sun). Superimposed on the photovoltaic response curves in the figure are the water electrolysis current densities for one, or two series intercon-

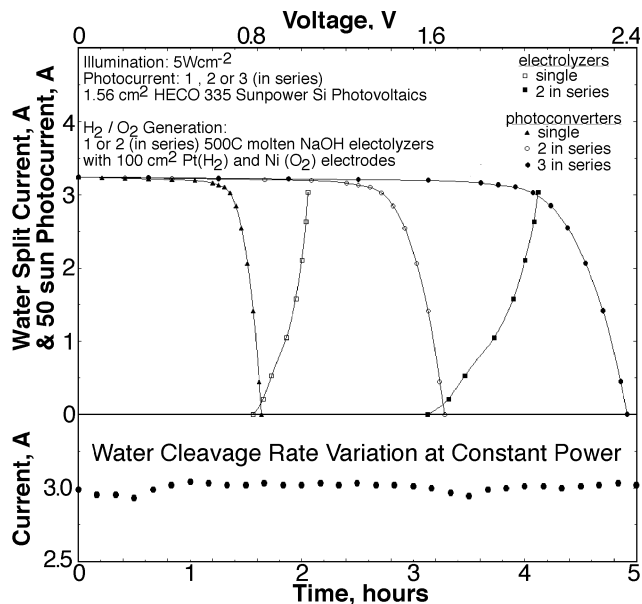


Fig. 3 Photovoltaic and electrolysis charge transfer for thermal electrochemical solar driven water splitting. Photocurrent is shown for 1, 2 or three 1.561 cm^2 HECO 335 Sunpower Si photovoltaics in series at 50 suns. Photovoltaics drive 500°C molten NaOH steam electrolysis using Pt gauze anode and cathodes. Inset: electrolysis current stability.

ected, 500°C molten NaOH single compartment cell configuration electrolyzers.

Constant illumination, generates for the three series cells, a constant photopotential for stability measurements at sufficient power to drive two series molten NaOH electrolyzers. At this constant power, and as presented in the lower portion of Fig. 3, the rate of water splitting appears fully stable over an extended period. In addition, as measured and summarized in the upper portion of the figure, for the overlapping region between the solid triangle and open square curves, a single Si photovoltaic can drive 500°C water splitting, albeit at an energy beyond the maximum power point voltage, and therefore at diminished efficiency. This appears to be the first case in which an external, single, small band gap photosensitizer can cleave water, and is accomplished by tuning the water splitting electrochemical potential to decrease below the Si open circuit photovoltage. $V_{\text{H}_2\text{O}}$ -tuned is accomplished by two phenomena: (i) the thermodynamic decrease of $E_{\text{H}_2\text{O}}$ with increasing temperature, and (ii) a partial recombination of the water splitting products. $V_{\text{H}_2\text{O}}$ -tuned can drive system efficiency advances, e.g. AlGaAs/GaAs, transmits more insolation, $E_{\text{IR}} < 1.4 \text{ eV}$, than Si to heat water, and with η_{photo} over 30% , prior to system engineering losses, calculates to over 50% η_{solar} to H_2 . Conceptual and fundamental details of splitting of the thermal and visible insolation, with the former to heat water for electrolysis, and the latter to drive electrical charge formation are discussed in our recent, related paper.⁸ This work was supported in part by Saxony-Israeli Fund, Energy ManLam and GM Funds.

Notes and references

- 1 A. Kogan, E. Spiegler and M. Wolfshtein, *Int J. Hydrogen Energy*, 2000, **25**, 739; J. Funk, *Int J. Hydrogen Energy*, 2001, **26**, 185.
- 2 J. Miyake, M. Miyake and Y. Adsada, *Solar Energy Mater.*, 1999, **70**, 89; E. Amouyal, *Solar Energy Mater.*, 1995, **249**, 38.
- 3 S. Khan, M. Al-Shahry and W. Ingler Jr., *Science*, 2002, **297**, 2243.
- 4 Z. Zou, Y. Ye, K. Sayama and H. Arakawa, *Nature*, 2001, **414**, 625.
- 5 A. Fujishima and K. Honda, *Nature*, 1972, **238**, 37.
- 6 S. Licht, B. Wang, S. Mukerji, T. Soga, M. Umeno and H. Tributsh, *J. Phys. Chem., B*, 2000, **104**, 8920; *ibid.*, 2001, **105**, 6281.
- 7 J. O'M. Bockris, *Energy Options*, Halsted Press, NY, 1980.
- 8 S. Licht, *J. Phys. Chem., B*, 2003, **107**, 4253.
- 9 E. Fletcher, *J. Solar Energy Eng.*, 2001, **123**, 143.